High-Strength Carbon Nanotube Fibers Fabricated by Infiltration and Curing of Mussel-Inspired Catecholamine Polymer

Seongwoo Ryu, Yuhan Lee, Jae-Won Hwang, Seonki Hong, Chunsoo Kim, Tae Gwan Park, Haeshin Lee,* and Soon Hyung Hong**

The authors express their sincere condolences to the family on the death of Prof. Tae Gwan Park

Carbon nanotubes (CNTs) have received extensive attention due to their extraordinary properties in electronic conduction,[1] heat transfer,[2] and mechanical strength.[3] Materials with unparallel performance, such as super-strong, lightweight e-textiles, can be fabricated from CNTs, suggesting a future revolution in materials science. Thus, the emerging CNT technology will largely depend on the development of effective spinning and post-spinning processes to realize such unprecedented materials. Two widely implemented strategies for fabricating CNT fibers are in-solution[4–7] and solid-state spinning techniques. The in-solution spinning of CNTs can produce continuous CNT fibers; however, homogeneous dispersion of CNTs in the solvent is necessary for proper spinning. Moreover, the properties of the CNT fibers strongly depend on the methods of CNT dispersion. An alternative strategy is solid-state spinning,[8–17] which allows avoidance of CNT dispersion in solvents and for various post-spinning processes to be applied with ease. Twisting,[10–16] densification,[9,18] and infiltration[8,19,20] are examples of post-spinning processes, and the main purpose of the spinning and post-spinning processes is to enhance the mechanical properties of CNT fibers. Despite the effort that has been made, however, fabrication of strong CNT fibers remains a great challenge.

S. Ryu, J.-W. Hwang, Prof. S. H. Hong
Korea Advanced Institute of Science & Technology (KAIST)
Department of Materials Science and Engineering
KAIST Institute for the NanoCentury
335 Science Rd. Daejeon, 305–701, South Korea
E-mail: shhong@kaist.ac.kr
Y. Lee, C. Kim, Prof. T. G. Park
Korea Advanced Institute of Science & Technology (KAIST)
Department of Biological Sciences
The Graduate School of NanoScience and Technology
KAIST Institute for the NanoCentury
335 Science Rd. Daejeon, 305–701, South Korea
S. Hong, Prof. H. Lee
Korea Advanced Institute of Science & Technology (KAIST)
Department of Chemistry
The Graduate School of NanoScience and Technology
KAIST Institute for the NanoCentury
335 Science Rd. Daejeon, 305–701, South Korea
E-mail: haeshin@kaist.ac.kr

DOI: 10.1002/adma.201004228

The strong protein-based adhesives found in marine mussel *Mytilus edulis*, provide an important insight into the development of post-spinning processes of CNT fibers. The mussel secretes special adhesive foot proteins that undergo rapid solidification in seawater. At a molecular level, the unusual amino acid 3,4-dihydroxy-L-phenylalanine (DOPA) found in the adhesive proteins functions as a molecule that is responsible for the solidification by oxidative chemical crosslinking.[21–24] From a chemical point of view, covalent crosslinking with amines and/or catechol (a side chain of DOPA) or metal coordination are the reactions involved with DOPA, and the reactions are responsible for mechanical reinforcement of the adhesive materials of mussels.[25] Here, inspired by the molecular mechanics of mussel adhesive formation, we demonstrate a new post-spinning process for the fabrication of CNT fibers (**Figure 1**a,b). By infiltration of mussel-mimetic adhesive polymers and curing through thermal and metal oxidation, we demonstrate an increase in the tensile strength of CNT fibers by up to 470%. The study described suggests a general post-spinning approach for enhancement of the mechanical properties of CNT fibers prepared by various spinning techniques.

Vertically well-aligned CNT arrays were grown on Fe-catalyst-immobilized (1.7-nm-thick) silicon substrates by plasma-enhanced chemical vapor deposition. Methane (CH_4) was used as the carbon source to synthesize CNTs, with argon (Ar), hydrogen (H_2), and oxygen (O_2) carrier gases. In the presence of Ar gas flow (100 sccm), temperature was raised up to 730 °C for 7 min, followed by Ar/H_2 gas (12 sccm) for 5 min. Finally, CH_4/O_2 gas (66/1 sccm) was provided in the presence of Ar/H_2 gas for 15 min. Scanning electron microscopy (SEM) analysis showed that the fully grown, vertically aligned CNT forest was 720 μm in height, interacting with neighboring CNTs by van der Waals forces (Figure S1, Supporting Information).[9] The CNT fibers (Figure 1d) directly spun from the CNT forest (Figure 1c) underwent the following steps of post-spinning processes: 1) the CNT fibers were mechanically twisted; 2) the adhesive polymer poly(ethylenimine) catechol (PEI-C) was infiltrated into the fibers; and 3) the CNT fibers were densified by solvent evaporation at 120 °C (Figure 1f). The densification, driven by surface tension, occurs during evaporation of methanol (Figure 1e). The diameter of loosely packed CNT fibers (Figure 1d, inset) was markedly decreased from 91.8 to 17.1 μm (Figure 1f, inset) as a result of the post-spinning

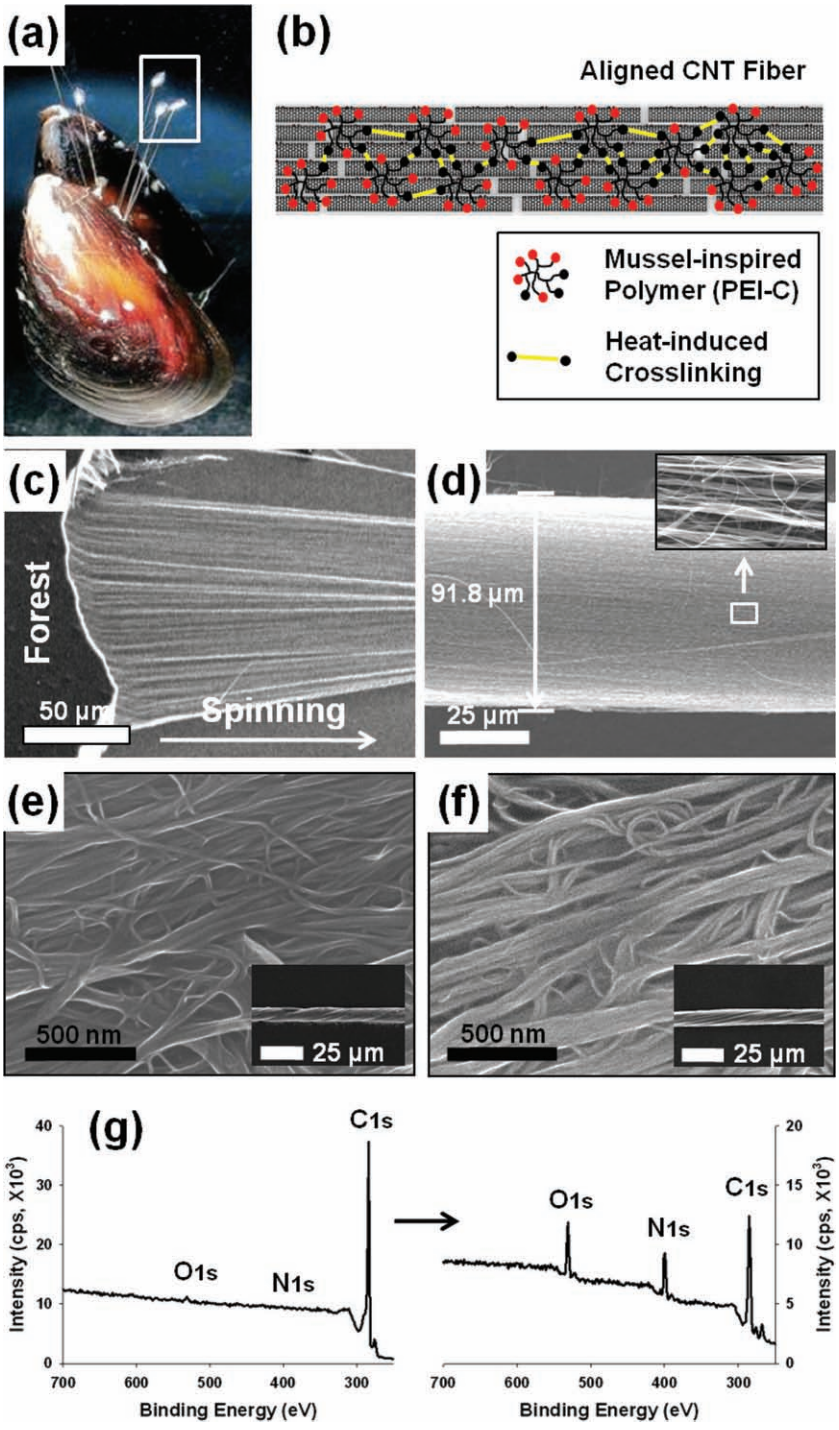

Figure 1. Fabrication and characterization of mussel-inspired CNT fibers. a) A photograph of a mussel attached to Si substrate. b) A schematic illustration of one-dimensionally aligned CNT fibers that are mechanically reinforced by mussel-mimetic, catechol-containing adhesives. c) Spinning CNT fibers from the forest. d) SEM image of the spun CNT fibers (scale bar: 25 μm) e,f) High magnification SEM images of e) densified CNT fiber and f) h-PEI-C treated CNT fiber. The insets show the SEM images of each CNT fiber sample. g) XPS spectra of CNT fibers before (left) and after (right) infiltration of PEI-C followed by thermal curing.

processes, twisting, infiltration, and densification. The decrease in diameter is primarily due to the solvent evaporation; the post-spinning process in the absence of PEI-C adhesives resulted in similar changes in diameter decreasing to 16.6 ± 3.0 μm (Figure 1e). X-ray photoelectron spectroscopy (XPS) analysis showed N 1s (≈400 eV) and O 1s (≈532 eV) peaks from the infiltrated PEI-C adhesives (Figure 1g, right panel). In contrast, no nitrogen (N 1s) was observed in the CNT fibers that were not treated with PEI-C adhesives (Figure 1g, left panel). The slight oxygen signal was due to the unavoidable surface oxidation of CNTs. Energy dispersive X-ray spectroscopy (EDS) analysis revealed similar nitrogen (25.3% for the outer and 22.9% for the inner region) and oxygen (17.4% for the outer and 16.2% for the inner region) compositions in the cross-sectioned CNT fiber (Figure S2 and Table S1, Supporting Information). This result indicated that the polymer was effectively diffused into the core region of the CNT fibers. The mass percentage of the PEI-C polymer in the CNT fiber was ≈8 wt%, determined by measuring changes in weight and volume utilizing a 3-m-long CNT fiber. These results clearly demonstrate that the mussel-inspired adhesive polymers are effectively diffused between the individual CNTs for mechanical reinforcement.

The PEI-C infiltrated CNT fibers exhibited 65% increase in tensile strength from 0.55 ± 0.11 GPa to 0.91 ± 0.24 GPa compared with the fibers without the adhesive treatment. When the infiltrated PEI-C molecules were crosslinked at 120 °C for 2 h, a significant enhancement in tensile strength and modulus was observed; the tensile strength increased from 0.91 ± 0.24 GPa to 2.2 ± 0.15 GPa and the modulus increased from 65 ± 17 GPa to 120 ± 23 GPa (**Figure 2**a). Considering the density of each sample (0.53 g cm^{-3} before infiltration and 0.55 g cm^{-3} after infiltration), the specific strength values were also increased from 1.04 ± 0.25 MN m kg^{-1} to 4.00 ± 0.27 MN m kg^{-1} (Table S2, Supporting Information). At high temperatures above 90 °C, catechols are oxidized to quinones that react with amine and/or catechol groups of nearby PEI-C by Michael-type addition and/or Schiff base formation.[26,27] At low temperatures below 40 °C, catechols do not exhibit chemical reactivity, resulting in a marginal increase in tensile strength to 0.91 ± 0.24 GPa. To further verify the catechol-mediated crosslinking reactions, the infiltrated PEI-C adhesives were retrieved by acid treatment (5 M HCl), as reported previously;[28] the UV-vis spectra showed a broad peak at 320 nm in addition to the unoxidized catechol peak at 280 nm, indicating oxidative crosslinking of the PEI-C polymers (Figure 2b).[29] In addition, calorimetric analysis using

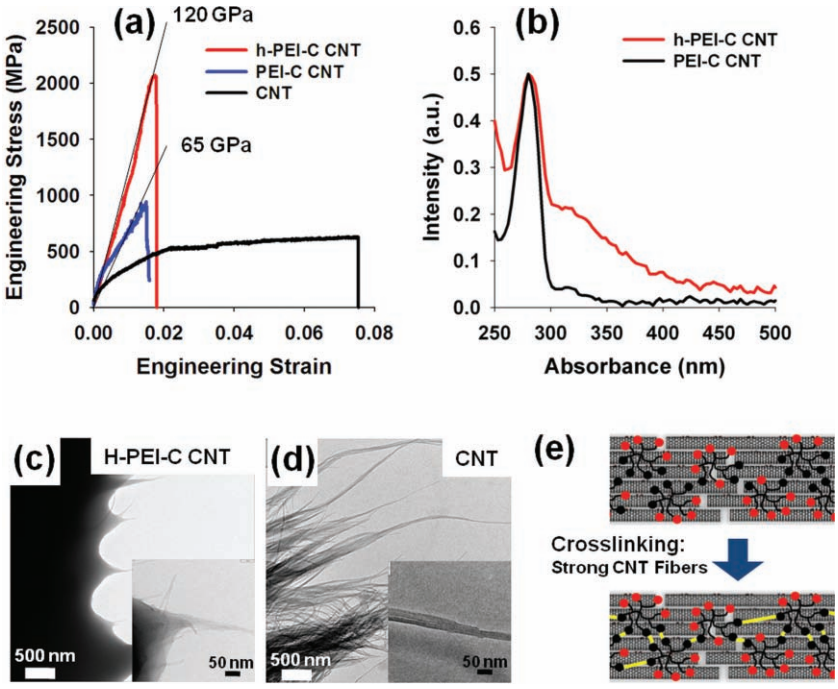

Figure 2. Mechanical reinforcement of the CNT fibers. a) Force–distance curves of methanol-densified CNT fibers (control; black), PEI-C1-infiltrated (blue), and heat-treated PEI-C1-infiltrated CNT fibers (red). b) UV-vis spectra of PEI-C retrieved from CNT fibers before (black) and after (red) thermal treatment. c,d) TEM fractography images of PEI-C infiltrated CNT fibers after c) methanol densification and d) heat treatment. e) A schematic illustration of the reinforcement of the CNT fibers.

differential scanning calorimetry (DSC) also revealed that an endothermal peak of PEI-C at 55 °C, which is an indication of a crosslinking reaction between PEI-Cs, was significantly lower in the subsequent temperature scanning. The data suggest that the strong covalent linkages between PEI-Cs were formed upon heating (Figure S3, Supporting Information). As for CNT and PEI-C interactions, π–π bonds between catechol and CNTs, as well as hydrogen bonds between the amine of PEI and hydroxyl or epoxide groups of the CNTs, might be involved. Furthermore, ^{1}H NMR spectroscopy clearly showed complex oxidation of catechol in the CNT fibers. The downfield shift, increased number, and broadness of the proton peaks demonstrated oxidative catechol–catechol crosslinking upon heating (Figure S4, Supporting Information). Transmission electron microscopy (TEM) analysis of the fractured fibers provided insight into the mechanical reinforcement by PEI-C adhesives; the presence of a bundle-shaped fracture (Figure 2c) rather than a hairy-type failure (Figure 2d) indicates an important role of PEI-C in adhesion between CNTs (Figure 2e). In general, for linearly aligned CNT fibers, inter-nanotube friction is a primary interaction against applied strain force, which determines strength of the fiber.[30] Sliding between individual CNT occurs when the strain force is greater than the friction force. In this case, a hairy-type failure shown in Figure 2d was often observed due to the sliding of individual CNTs. However, the hairy-type failure was not observed for the CNT fibers treated by PEI-C adhesive. A localized, bundle-shaped fracture was detected in which an individual CNT was tightly bound by the infiltrated adhesive (Figure 2c).

PEI-Cs with various degrees of catechol conjugations were prepared and labeled as PEI-C1 for 25.0%, PEI-C2 for 13.5%, and PEI-C3 for 5.0% conjugation to the primary amine groups of PEI. The degree of catechol conjugation of PEI-Cs and the tensile strength of the CNT fibers showed a positive correlation: 0.6 ± 0.13 GPa for PEI-C3, 1.37 ± 0.37 GPa for PEI-C2, and 2.2 ± 0.37 GPa for PEI-C1 (**Figure 3**a and Table S3, Supporting Information). The effective mechanical reinforcement is due to increased crosslinking between the adhesive polymers that are strongly adhered to the surface of individual CNTs. In fact, UV-vis spectra of PEI-C1, PEI-C2, and PEI-C3 obtained from the CNT fibers showed increased catechol crosslinking at 320 nm (Figure S5, Supporting Information). The mechanical properties are also dependent on the molecular weight of the adhesives. A low-molecular-weight (≈500 Da) adhesive that is structurally similar to PEI-C (sPEI-C) was synthesized. The CNT fibers fabricated by sPEI-C showed an early-state failure (Figure 3a, purple), indicating the importance of the molecular weight of the adhesives. This result strongly suggests that the facile diffusion caused by low molecular weight is not an important factor for mechanical reinforcement of CNT fibers. Rather, a large number of catechols per chain that can effectively interconnect the CNTs are the critical aspect to enhance the tensile strength of CNT fibers. Unexpectedly, the sPEI-C treatment resulted in a softening of the fiber and exhibiting the highest strain, about 2.5%, among the tested CNT fibers.

The crystallinity of infiltrated polymers has been another consideration for enhancement of mechanical properties. Poly(vinyl alcohol) (PVA)–CNT composites fabricated by in-solution and solid-state spinning techniques are well-known examples.[4,6,8] Crystallization of the surface-adsorbed PVA molecules found in the vicinity of CNTs greatly influences the mechanical properties of CNT fibers. In fact, by catechol conjugation, the non-crystalline PEI was converted to a crystalline polymer (Figure 3b); two broad peaks at $2\theta = 12.5°$ and 25° suggest the newly generated crystalline nature of PEI-C.

Fe(II/III) ions play an important role in reinforcing the mechanical strength of the mussel adhesives.[17,31,32] The Fe–catechol coordination and Fe-induced oxidative crosslinking chemistry could provide a strategy to further enhance mechanical properties of CNT fibers (Figure 3c,d). To maximize the degree of mechanical reinforcement of the CNT fibers, the PEI-C1-infiltrated CNT fibers were further treated with 0.5 M $Fe(NO_3)_3$ solution for 10 min. The tensile strength of iron-treated CNT fibers was further increased up to 2.5 ± 0.31 GPa with the similar modulus before Fe(III) treatment (Figure 3c). The UV-vis spectra of the metal-polymer-CNT fibers showed evidence of iron-induced catechol crosslinking (Figure 3d). In a previous study, catechol could form coordination bonds with Fe(III), generating three distinct

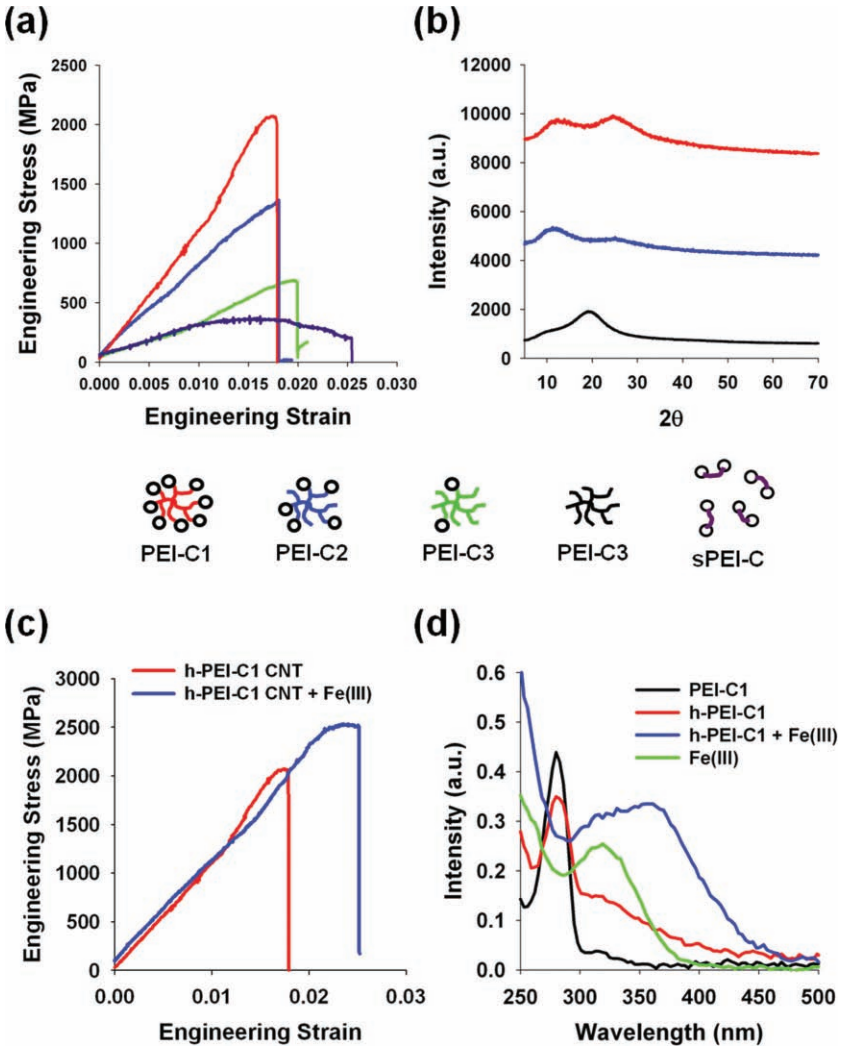

Figure 3. Engineering mussel-inspired adhesives influence the mechanical properties of CNT fibers. a) The tensile strength of CNT fibers was increased as the degree of catechol conjugation onto the PEI polymer backbone was increase. The number of catechols per PEI molecule: PEI-C1 (red) > PEI-C2 (blue) > PEI-C3 (green). Stress–strain curves of CNT fibers infiltrated by catechol-conjugated oligoamine (h-sPEI-C) (purple). b) XRD spectra of PEI (black), h-PEI-C2 retrieved from fibers (blue), and h-PEI-C1 (red). c) Stress–strain curves of h-PEI-C1 CNT (red) and h-PEI-C1+Fe(III) (blue). d) UV-vis spectra of PEI-C1 (black), h-PEI-C1 (red), and h-PEI-C1+Fe(III) (blue) retrieved from CNT fibers. $Fe(NO_3)_3$ in aqueous solution (green) was used for comparison.

coordination species: 1:1 (Fe:catechol, mono, weak bands at 429 and 700 nm), 1:2 (bis, strong band at 470 nm), and 1:3 (tris, strong band at 590 nm) complexes.[31] In this study, a broad peak from 320 to 500 nm appeared, which was distinct from the spectrum of $Fe(NO_3)_3$ aqueous solutions, and the unoxidized catechol peak at 280 nm decreased simultaneously after addition of Fe(III). Due to the high molecular weight of PEI (M_w = 25 kDa), the chemical environment of the conjugated catechols is intrinsically hetero-geneous, which results in the broad peak of catechol–Fe(III) coordination. The previous report utilizing catechol–Fe(III) coordination to produce a stiff organic thin film also did not show a distinct peak.[32] Recently, the molecular-level insight into the role of Fe (II/III) ions in the mussel threads was also reported.[33] Iron-mediated covalent crosslinking not only increased the tensile strength of the adhesive threads but also enhanced elasticity, proposing a general principle of mussel-inspired control of mechanical properties by iron and catechol chemistry.

In conclusion, a method to reinforce the mechanics of CNT fibers inspired by the strategy found in the formation of mussel threads was reported. The four-step sequential fabrication processes that consist of 1) spinning and twisting, 2) mussel-mimetic adhesive infiltration, 3) temperature-induced crosslinking, and 4) Fe(III)-mediated catechol crosslinking resulted in a remarkable ≈500% increase of the tensile strength of the CNT fibers with a reduction in the ductility of the fiber compared to untreated CNT fibers. The super-strong CNT fibers had a diameter of 15–20 μm, which is larger than reported CNT fibers with the tensile strength greater than 2 GPa, indicating fewer defects in the approach described here. Thus, the mechanical reinforcement achieved by treatment of the mussel-inspired adhesive suggests a new possibility to enhance mechanical properties of other carbon nanocomposite materials. However, compared to pristine CNT, the modulus and strength of the CNT fiber was small[34] and, therefore, efforts to improve the mechanics of CNT fibers should be continued.

Supporting Information

Supporting Information is available from the Wiley Online Library or from the author.

Acknowledgements

S.R. and Y.L. contributed equally to this work. The authors acknowledge financial support from the Center for Nanostructured Materials Technology under the 21st Century Frontier R&D Programs of the Ministry of Education, Science and Technology, Korea (2010K000275, S.H.H), Future-based Technology Development Program (Nano Fields) through the National Research Foundation of Korea (NRF) funded by the Ministry of Education, Science and Technology (2010–0019132, S.H.H), WCU/Korea Biotech R&D Programs (R31-10071-0/2010K001356, T.G.P., H.L.), and KI NanoCentury (S.H.H, T.G.P., H.L.) in Korea.

Received: November 16, 2010
Revised: January 3, 2011
Published online: March 15, 2011

[1] A. Javey, J. Gue, Q. Wang, M. Lundstrom, H. Dai, *Nature* **2003**, *424*, 654.
[2] M. F. Yu, B. S. Files, S. Arepalli, R. S. Ruoff, *Phys. Rev. Lett.* **2000**, *84*, 5552.

[3] M. F. Yu, O. Lourie, M. J. Dyer, K. Moloni, T. F. Kelly, R. S. Ruoff, *Science* **2000**, *287*, 637.
[4] B. Vigolo, A. Pénicaud, C. Coulon, C. Sauder, R. Pailler, C. Journet, P. Bernier, P. Poulin, *Science* **2000**, *290*, 1331.
[5] L. M. Ericson, H. Fan, H. Peng, V. A. Davis, W. Xhou, J. Xulpizio, Y. Wang, R. Booker, J. Vavro, C. Guthy, A. N. G. Parra-Vasquez, M. J. Kim, S. Ramesh, R. K. Saini, C. Kittrell, G. Lavin, H. Schmidt, W. W. Adams, W. E. Billups, M. Pasquali, W. F. Hwang, R. H. Hauge, J. E. Fischer, R. E. Smally, *Science* **2004**, *305*, 1447.
[6] A. B. Dalton, S. Collins, E. Muñoz, J. M. Razal, V. H. Ebron, J. P. Ferraris, R. H. Baughman, *Nature* **2003**, *423*, 703.
[7] M. E. Kozlov, R. C. Capps, W. M. Sampson, V. H. Ebron, J. P. Ferraris, R. H. Baughman, *Adv. Mater.* **2005**, *17*, 614.
[8] M. Zhang, K. R. Atkinson, R. H. Baughman, *Science* **2004**, *306*, 1358.
[9] X. Zhang, K. Jiang, C. Feng, P. Liu, L. Zhang, J. Kong, T. Zhang, Q. Li, S. Fan, *Adv. Mater.* **2006**, *18*, 1505.
[10] X. Zhang, Q. Li, T. G. Holesinger, P. N. Arendt, J. Huang, P. D. Kirven, T. G. Clapp, R. F. DePaula, X. Liao, Y. Zhao, L. Zheng, D. E. Petereson, Y. Zhu, *Adv. Mater.* **2007**, *19*, 4198.
[11] X. Zhang, Q. Li, Y. Tu, Y. Li, J. Y. Coulter, L. Zheng, Y. Zhao, Q. Jia, D. E. Peterson, Y. Zhu, *Small* **2007**, *2*, 244.
[12] Y. Nakayama, *Jpn. J. Appl. Phys.* **2008**, *47*, 8149.
[13] Y. L. Li, L. A. Kinloch, A. H. Windle, *Science* **2004**, *304*, 276.
[14] K. Koziol, J. Vilatela, A. Moisala, M. Motta, P. Cunniff, M. Sennett, A. Windle, *Science* **2007**, *318*, 1892.
[15] L. Ci, N. Punbusayakul, J. Wei, R. Vajtai, S. Talapatra, P. M. Ajayan, *Adv. Mater.* **2007**, *19*, 1719.
[16] L. Zheng, X. Zhang, Q. Li, S. B. Chikkannanavar, Y. Li, Y. Zhao, X. Liao, Q. Jia, S. K. Doorn, D. E. Peterson, Y. Zhu *Adv. Mater.* **2007**, *19*, 2567.
[17] K. Jiang, Q. Li, S. Fan, *Nature* **2002**, *419*, 801.
[18] W. Ma, L. Liu, Z. Zhang, R. Yang, G. Liu, T. Zhang, X. An, X. Yi, Y. Ren, Z. Niu, J. Li, H. Dong, W. Zhou, P. M. Ajayan, S. Xie, *Nano Lett.* **2009**, *9*, 2855.
[19] K. Liu, Y. Sun, R. Zhou, H. Zhu, J. Wang, L. Liu, S. Fan, K. Jiang, *Nanotechnology* **2010**, *21*, 045708.
[20] K. Liu, Y. Sun, X. Lin, R. Zhou, J. Wang, S. Fan, K. Jiang, *ACS Nano* **2010**, *4*, 5827.
[21] N. H. Andersen, T. E. Mates, M. S. Toprak, G. D. Stucky, F. W. Zok, J. H. Waite, *Langmuir* **2009**, *25*, 3323.
[22] S. Haemers, M. C. Leeden, G. Frens, *Biomaterials* **2005**, *26*, 1231.
[23] H. Lee, N. F. Scherer, P. B. Messersmith, *Proc. Natl. Acad. Sci. USA* **2006**, *103*, 12999.
[24] N. H. Andersen, G. E. Fantner, S. Hohlbauch, J. H. Waite, F. W. Zok, *Nat. Mater.* **2007**, *6*, 669.
[25] S. W. Taylor, D. B. Chase, M. H. Emptage, M. J. Nelson, J. H. Waite *Inorg. Chem.* **1996**, *35*, 7572.
[26] J. H. Waite, *Comp. Biochem. Physiol.* **1990**, *97*, 19.
[27] K. Li, X. Geng, J. Simonsen, J. Karchesy, *Int. J. Adhes. Adhesives* **2004**, *24*, 327.
[28] S. M. Kang, J. Rho, I. S. Choi, P. B. Messersmith, H. Lee, *J. Am. Chem. Soc.* **2009**, *131*, 13224.
[29] B. P. Lee, J. L. Dalsin, P. B. Messersmith, *Biomacromolecules* **2002**, *3*, 1038.
[30] N. Behabtu, M. J. Green, M. Pasquali, *Nano Today* **2008**, *3*, 24.
[31] S. W. Taylor, G. W. Luther III, J. H. Waite, *Inorg. Chem.* **1994**, *33*, 5819.
[32] P. Podsiadlo, Z. Liu, D. Paterson, P. B. Messersmith, N. A. Kotov, *Adv. Mater.* **2007**, *19*, 949.
[33] M. J. Harrington, A. Masic, N. Holten-Anderson, J. H. Waite, P. Fratzl, *Science* **2010**, *328*, 216.
[34] B. Peng, M. Locascio, P. Zapol, S. Li, S. L. Mielke, G. C. Schatz, H. D. Espinosa, *Nat. Nanotechnol.* **2008**, *3*, 626.